Permeability Transition Pore-Mediated Mitochondrial Superoxide Flashes Mediate an Early Inhibitory Effect of Aβ1–42 on Neural Progenitor Cell Proliferation

Yan Hou[1], **Paritosh Ghosh**[2], **Ruiqian Wan**[1], **Xin Ouyang**[1], **Heping Cheng**[3], **Mark P. Mattson**[1,4,*], and **Aiwu Cheng**[1,*]

[1]Laboratory of Neurosciences, National Institute on Aging Intramural Research Program, Baltimore, MD 21224

[2]Laboratory of Immunology, National Institute on Aging Intramural Research Program, Baltimore, MD 21224

[3]Institute of Molecular Medicine and National Laboratory of Biomembrane and Membrane Biotechnology, Peking University, Beijing 100871, China

[4]Department of Neuroscience, Johns Hopkins University School of Medicine, Baltimore, MD 21205

Abstract

Cellular damage by reactive oxygen species (ROS) and altered neurogenesis are implicated in the etiology of AD and the pathogenic actions of amyloid β-peptide (Aβ); the underlying mechanisms and the early oxidative intracellular events triggered by Aβ are not established. In the present study, we found that mouse embryonic cortical neural progenitor cells exhibit intermittent spontaneous mitochondrial superoxide (SO) flashes that require transient opening of mitochondrial permeability transition pores (mPTPs). The incidence of mitochondria SO flash activity in NPCs increased during the first 6 – 24 hours of exposure to aggregating amyloid β-peptide (Aβ1-42), indicating an increase in transient mPTP opening. Subsequently, the SO flash frequency progressively decreased and ceased between 48 and 72 hours of exposure to Aβ1-42, during which time global cellular ROS increased, mitochondrial membrane potential decreased, cytochrome C was released from mitochondria and the cells degenerated. Inhibition of mPTPs and selective reduction in mitochondrial SO flashes significantly ameliorated the negative effects of Aβ1-42 on NPC proliferation and survival. Our findings suggest that mPTP-mediated bursts of mitochondrial SO production is a relatively early and pivotal event in the adverse effects of Aβ1-42 on NPCs. If Aβ inhibits NPC proliferation in the brains of AD patients by a similar mechanism, then interventions that inhibit mPTP-mediated superoxide flashes would be expected to protect NPCs against the adverse effects of Aβ.

Keywords

*Corresponding authors: Mark P. Mattson (mattsonm@grc.nia.nih.gov) and Aiwu Cheng (chengai@mail.nih.gov), Laboratory of Neurosciences, National Institute on Aging Intramural Research Program, 251 Bayview Blvd, Baltimore, MD 21224.

1. Introduction

Alzheimer's disease (AD) involves progressive synaptic dysfunction and death of neurons in brain regions critical for learning and memory processes. It is characterized histopathologically by the accumulation of extracellular plaques comprised of amyloid β-peptide (Aβ) and intracellular neurofibrillary tangles which are aggregates of the microtubule-associated protein tau (Goedert and Spilantini, 2006). Genetic, clinical and experimental findings have pointed to altered proteolytic processing of the β-amyloid precursor protein (APP), which increases the production of neurotoxic forms of Aβ (particularly Aβ1-42), as being central to the disease process (Klein et al., 2001; Mattson, 2004). A critical role for Aβ production, self–aggregation and neurotoxicity in AD is suggested by genetic studies that identified mutations in APP and presenilin-1/γ-secretase as the cause of many cases of early-onset dominantly inherited AD and by investigations of animal and cell culture models of AD (Mattson, 2004; Hardy, 2006). The neuronal degeneration mechanisms both upstream and downstream of Aβ1-42 involve oxidative stress and impaired cellular energy metabolism (Gabuzda et al., 1994; Mattson, 2004; Tamagno et al., 2008; Jo et al., 2010; Gwon et al., 2012), suggesting prominent roles for mitochondrial alterations in the disease process. Aβ may promote mitochondrial dysfunction in neurons in AD because exposure of cultured neurons to Aβ results in decreased ATP production and increased mitochondrial calcium uptake that can trigger opening of the mitochondrial permeability transition pores (mPTPs) and apoptosis (Keller et al., 1998; Hashimoto et al., 2003; Keil et al., 2004). However, the early intracellular events that mediate Aβ-induced disruption of mitochondrial function and cellular dysfunction remain elusive. During the process of self-aggregation on the surface of neurons, Aβ generates reactive oxygen species (ROS) which cause membrane lipid peroxidation, impair synaptic function and render neurons vulnerable to calcium overload (Hensley et al., 1994; Mark et al., 1997; Huang et al., 1999; Bonda et al., 2010, Shankar et al., 2007). In addition, Aβ can impair mitochondrial function in neurons by a ROS-mediated mechanism that can be attenuated by overexpression of manganese superoxide dismutase (Mn-SOD) (Keller et al., 1998) and exacerbated by Mn-SOD deficiency (Esposito et al., 2006).

Emerging evidence suggests that neurogenesis may be important for the maintenance of learning and memory during aging (Ma et al., 2009; Bizon et al., 2004; Dupret et al., 2008), and that neurogenesis is abnormally impaired in AD (Lazarov et al., 2010). The proliferation and survival of neural progenitor cells (NPCs) in the dentate gyrus of the hippocampus is reduced in mice transgenic for a mutated form of APP that causes early-onset familial AD (Haughey et al., 2002). Similar results were obtained in studies of other mouse models of AD (Verret et al., 2007; Zhang et al., 2007; Demars et al., 2010), suggesting that abnormalities in NPCs might contribute to the pathogenesis of AD. However, the mechanism by which Aβ adversely affects the proliferation and survival of NPCs is unknown.

We previously developed a novel mitochondria-targeted fluorescent superoxide anion radical (SO) indicator (mt-cpYFP) to demonstrate the existence of spontaneous bursts of mitochondrial SO production (SO flashes) in different types of excitable cells that were dependent upon both electron transport and the transient opening of mPTP (Wang et al., 2008). Recently, we used mt-cpYFP to show that self-renewing NPCs exhibit intermittent SO flashes that are also generated by a mechanism involving the functional coupling of transient mPTP opening with a rapid burst of SO generation; the flash frequency increases during the switch of NPCs from proliferation to differentiation (Hou et al., 2012). In the present study, we found that an increased frequency of SO flashes is an early mitochondrial response to Aβ1–42 that inhibits proliferation of NPCs. Moreover, prolonged exposure of

NPCs to Aβ1–42 results in a SO-mediated sustained global elevation of ROS that results in cell death. Our findings demonstrate a pivotal role for mPTP-mediated SO generation in the adverse effects of Aβ on NPCs, and suggest a potential therapeutic application of treatments that normalize mitochondrial mPTP opening and SO production.

2. Methods

2.1. Primary neural progenitor cell cultures, treatments and cell transfection

NPCs isolated from embryonic mouse cerebral cortex were propagated as free-floating aggregates (neurospheres) to promote self-renewal of NPCs for use in experiments as described previously (Cheng et al., 2007; Hou et al., 2012). Briefly, the telencephalon from embryonic day 14–16 mice was dissected in sterile Ca^{2+}- and Mg^{2+}-free Hanks' balanced saline solution (HBSS). The collected cortical tissue was incubated in 0.05% trypsin-EDTA in HBSS for 15 min at 37°C and then transferred to neurosphere (NS) culture medium consisting of Dulbecco's modified Eagle's medium (DMEM)/F12 (1:1) supplemented with B-27 (InVitrogen, Carlsbad, CA), 40 ng/ml basic fibroblast growth factor (bFGF; Becton Dickson, Bedford, MA) and 40 ng/ml epidermal growth factor (EGF; InVitrogen). These culture conditions were used for all experiments in this study. After dissociation by titration using a fire-polished Pasteur pipette, the cells were cultured at a density of 2×10^5 cells/ml in uncoated plastic culture flasks. The neurospheres that formed during 3 days in culture were dissociated and plated in polyethylenimine (PEI) coated dishes in MEM containing 10% fetal bovine serum (MEM+) for 1.5 h. The MEM+ was then replaced with NS culture medium. In PEI-coated dishes, the NPCs gradually spread across the growth substrate to form monolayer NPC cultures. All the experiments were performed in cultured NPC monolayers on culture day 4; the different treatments were administered beginning on culture days 2, 3 or 4 to generate different treatment time points (24, 48 and 72h) (Supplemental Fig. 1). Experimental treatments included the following: Tiron, TMP, MitoTEMPO, and cyclosporin A (Sigma, St. Louis, MO) which were prepared as 500–1000x stocks in dimethylsulfoxide or distilled water. Mitochondria-targeted tetrapeptide SS31 was synthesized as described previously (Cho et al., 2007). Aβ1-42 was purchased from Bachem (Torrance, CA). Treatments were administered by direct dilution into the culture medium, and an equivalent volume of vehicle was added to control cultures. Aβ1-42 oligomers were freshly prepared before treatment by dissolving the peptide in distilled water at a concentration of 200 μM. This stock solution was incubated at 37°C for 24 hours to promote peptide self-aggregation as indicated by the presence of Aβ1-42 oligomers (Supplemental Fig. 2). In some experiments, freshly prepared Aβ1-42 monomers were used as a control treatment. NPCs were transfected with plasmid of mt-cpYFP in pcDNA3.1 vector and the NPCs expressing mt-cpYFP were imaged 48 hours after transfections.

2.2. Confocal imaging of mitochondrial superoxide flashes

NPCs were transfected with 2 μg pcDNA3.1 plasmid containing mt-cpYFP coding sequence using FuGENE 6 reagent (Roche) according to the instructions of the manufacturer. The imaging was performed 48–72 h after transfection. Cells were imaged using a Zeiss LSM 510 confocal microscope with a 63X, 1.3NA oil immersion objective and a sampling rate of 1.5 s/frame. Dual excitation imaging of mt-cpYFP was achieved by alternating excitation at 405 and 488 nm and emission at 505 nm. Imaging experiments were performed at room temperature (24–26°C). Digital image processing used the Zeiss LSM 510 and sigma plot software (Research Systems), and user-designed programs.

2.3. Cell proliferation and cell death assays

After NPC cultures were exposed to experimental treatments for designated time periods, bromodeoxyuridine (BrdU) was added to the cultures at a final concentration of 10 μM, and

2 h later the cells were fixed in 4% paraformaldehyde in PBS. The cells were then incubated in a solution of 2 N HCl for 45 min and then cell membranes were permeabilized during a 30 min incubation in blocking solution (10% normal goat serum in PBS) containing 0.2% Triton X-100, and then incubated overnight with a primary antibody diluted in blocking solution at 4°C. Cells were washed with PBS and incubated with secondary antibodies diluted in blocking solution for 2 h at room temperature. The cells were counterstained with propidium iodide (PI) (0.02% PI and 1% RNAse in PBS) for 10 min; they were then washed with PBS and mounted on microscope slides in a fluorescence anti-fade medium (Vector Laboratories, CA). Images were acquired in five randomly chosen microscope fields using a 25X objective and dual channels for BrdU immunostaining (488 nm excitation and 510 nm emission) and propidium iodide (543 nm excitation and 590 nm emission). The BrdU- and propidium iodide-positive cells were counted simultaneously in each image, and the proliferation index was calculated as the number of BrdU-positive cells divided by the total number of the cells (propidium iodide-positive). A minimum of 3 cultures for each condition were used in each experiment. For neurosphere clonal analysis, primary NS were dissociated using a NeuroCult cell dissociation kit (StemCell Technologies) and plated into 96-well plates (Nunc) at 2000 cells per well in NS culture medium. Analyses were performed at 5–7 days in culture; images of NS were acquired from 8 wells per experimental condition and were then analyzed using Adobe Photoshop or NIH Image J software to quantify both the number of NS and the diameter of individual NS.

For cell death assays, NS were dissociated into single cells and plated in PEI-coated 96-well plates at a density of 5000 cells/well. Twenty four hours after plating, the cells were exposed to experimental treatments for designated time periods and culture medium was collected, and lactate dehydrogenase (LDH) activity levels in medium samples were quantified using a commercially available kit (Sigma). For cell death analysis, cells were fixed in 4% paraformaldehyde in PBS for 30 min at room temperature and then washed with PBS and stained with the DNA-binding dye Hoechst 33258 (5 μg/ml) in PBS for 2 h at room temperature or overnight at 4°C. Stained cells were examined with a confocal microscope using a 40X objective lens; cells were considered apoptotic if their nuclear chromatin was condensed or fragmented, and were considered viable if their chromatin was diffused and evenly distributed throughout the nucleus. All data presented are the results of 3–4 separate experiments.

2.4. Immunoblot analysis

Cultured cells were solubilized in sodium dodecyl sulfate–polyacrylamide gel electrophoresis sample buffer, and the protein concentration in each sample was determined using a Bio-Rad protein assay kit (Bio-Rad, Hercules, CA, USA) with bovine serum albumin as the standard. Proteins (30 μg of protein per lane) were then resolved in a 7.5–10% sodium dodecyl sulfate–polyacrylamide gel and electrophoretically transferred to a nitrocellulose membrane. For detecting Aβ1-42 oligomer formation, Aβ1-42 peptides that were either freshly dissolvedor incubated for 24 hour to enable peptide aggregation, were boiled and loaded into a 4–12% tris-glycerol gradient gel for electrophoresis. Membranes were blocked with 4% non-fat milk in TBST (Tris–HCl based buffer with 0.2% Tween 20, pH 7.5), and then incubated in the presence of primary antibody overnight at 4°C. Cells were then incubated for 1 h in the presence of a 1:5000 dilution of secondary antibody conjugated to horseradish peroxidase (Jackson Immunoresearch Laboratory). Reaction product was visualized using an Enhanced Chemiluminescence western blot detection kit (Amersham Bioscience, Piscataway, NJ). The blots were probed with antibodies against total or phosporylated extracellular signal-regulated kinase (ERK) 1/2, total or phosporylated p38, and total or phosphorylated JNK (Cell Signaling Biotechnology), Aβ (rabbit, 1:500, Life Technologies), or actin (mouse, 1:5000; Sigma).

2.5. Mitochondrial oxygen consumption

Oxygen consumption was determined using the BD Oxygen Biosensor System (BD Biosciences) as described previously (Schieke et al., 2006). NS were resuspended in culture medium and subsequently transferred to a 96-well plate where the same numbers of cells (1×10^6) were placed in each well. Levels of oxygen consumption were measured under baseline conditions and in the presence of FCCP (1 μM) or oligomycin (0.2 μg/ml). Fluorescence was recorded using a GENios multimode reader (Tecan, San Jose, CA) at 2-min intervals up to 2 h at an excitation of 485 nm and emission of 630 nm. For semiquantitative data analysis the maximum slope of fluorescence units/sec was used and converted into arbitrary units. The respiration rates shown are triplicate determinations of a single experiment that are representative of at least three similar experiments.

2.6. Mitochondrial membrane potential and cellular ROS measurements

To measure mitochondrial membrane potential, the mitochondrial membrane potential-sensitive fluorescent indicator chloromethyl-X-rosamine (CMXRos) was added to NPC cultures that had been treated with vehicle or 1μM Aβ1-42 oligomers. The cultures were incubated at 37°C for 20 min prior to imaging CMXRos fluorescence. To measure net intracellular accumulation of ROS, the peroxide-sensitive fluorescent probe 5-(and-6)-carboxy-2′7′-dichlorodihydrofluorescein diacetate (DCF; Invitrogen/Molecular Probes) was used. In brief, DCF was added to cultures that had been treated with vehicle or 1 or 5 μM Aβ1-42. The cultures were incubated at 37°C for 30 min. After washing with pre-warmed NPC culture medium, images of cells were acquired using a 60X objective on an Olympus confocal microscope. The excitation and emission wavelengths for Mitotracker red (CMXRos) were 510 and 590 nm, respectively, and for DCF were 488 and 510 nm, respectively. The fluorescence intensities of approximately 500 cells per condition were quantified.

2.7. Data analysis

All data are presented as mean ± SD. Statistical analysis was performed by one-way ANOVA or two-way ANOVA where appropriate, followed by Bonferroni post hoc test for pairwise comparisons. P<0.05 was considered to be statistically significant.

Results

3.1. Exposure of NPCs to an Aβ1–42 oligomer-containing preparation results in an early increase of SO flash activity, and a subsequent diminution of SO flashes concurrent with elevated global ROS

NPC cultures were established from embryonic day 14.5 mouse cerebral neuroepithelium and propagated as free-floating neurospheres (NS), or dissociated and plated at a high density in polyethyleneimine-coated dishes for use in experiments (Cheng et al., 2007; Lathia et al., 2008). Evaluation of NS formation and growth, and quantification of mitochondrial SO flashes were performed as described previously (Hou et al., 2012). In NPC expressing the SO biosensor mt-cpYFP, fluorescence seen at 488 nm excitation was confined to the mitochondria as characterized previously (Hou et al., 2012) (Fig. 1A and B). To determine whether Aβ1–42 affects mitochondrial SO flash generation, we treated cortical NPCs with Aβ1–42 that had been preincubated for 24 hours to initiate and propagate peptide self-aggregation as indicated by the presence of peptide oligomers (Supplemental Fig. 2). Mitochondrial SO flashes were then imaged at designated time points. Examination of NPCs 24 hours after treatment suggested that more NPCs exhibited SO flashes in cultures exposed to 0.5 μM of the Aβ1-42 oligomer-containing preparation (OCP) compared to control cultures (Fig. 1A–1D). Significantly more cells exposed to 0.5 μM Aβ1–42 OCP exhibited a

repetitive pattern of SO flash generation compared to control cells (data not shown). Time course analysis of SO flashes suggested that they are random events among cells within a population such that an SO flash in one cell does not affect the probability of a flash in adjacent cells (Supplemental movies 1A and 1B). We further determined the percentage of NPCs exhibiting flashes during a 150 second recording period and found that 0.5, 1 or 5 μM Aβ1-42 OCP all resulted in a significant increase in SO flash incidence compared to control cultures (One way ANOVA: $F_{(3, 8)} = 4.32$, p=0.04; post-hoc Bonferroni test: **p<0.001 and * p<0.05, respectively, Fig. 1E). We found that 0.5 μM Aβ1-42 OCP generated the maximal effect on flash incidence and there were no further statistically significant increases in flash incidences with 1 or 5 μM Aβ1-42 OCP although there was a trend towards dose dependence (post-hoc Bonferroni test: 1 μM vs. 5 μM: p=0.63, Fig. 1E). NPCs treated with Aβ1–42 monomers 1μM and 5 μM did not show a change in SO flash incidence compared to control cultures (post-hoc Bonferroni test: p=0.55 (0 μM vs 1μM), p=0.87 (0 μM vs 5 μM), respectively, Fig. 1E).

The amplitude of individual SO flashes was not significantly affected by exposure to Aβ1–42 OCP (One way ANOVA: $F_{(3, 8)} = 1.75$, p=0.23; Fig. 1F). However, analysis of the kinetics of SO flashes (a total of 91 flashes analyzed) demonstrated a significantly shortened Tp (time to peak) in NPCs exposed to 1 and 5 μM Aβ1–42 OCP (One way ANOVA: $F_{(3, 8)} = 4.15$, p=0.047; post-hoc Bonferroni test: 1 μM vs. control: *p<0.05; 5μM vs. control: *p<0.05; Fig. 1G), and a prolonged T_{50} (50% decay time after the peak) in NPCs exposed to 5 μM Aβ1–42 OCP (One way ANOVA: $F_{(3, 8)} = 7.13$, p=0.01; post-hoc Bonferroni test: *p<0.05, Fig. 1H), indicating SO flash events with a more rapid initiation and a longer persistence compared to NPCs not exposed to Aβ1–42 OCP. Collectively, the findings show that exposure of NPCs to Aβ1–42 in the process of aggregation, as indicated by its containing oligomers, significantly increases the mitochondrial SO flash incidence during a 6–24 hour exposure period. In contrast, exposure of NPCs to 0.5, 1 μM and 5 μM Aβ1–42 OCP did not result in a significant increase in global ROS levels during a 24 h exposure period (One way ANOVA: $F_{(3,8)} = 1.47$, p=0.29; Fig. 1I).

We observed that exposure of NPCs to Aβ1-42 (OCP) resulted in an increase in SO flash frequency measured at 24 h. Because it was previously reported that Aβ1-42 OCP can damage and kill neurons (Klein et al., 2001; Mattson, 2004), we extended our analysis of SO flashes and their consequences for NPCs to time points beyond 24 hours. Whereas SO flash frequency was elevated at 24 h after exposure to Aβ1-42 OCP, SO flash frequency was significantly reduced approximately 50% below basal levels at 48 and 72 h after exposure to both 1 μM and 5 μM Aβ1-42 OCP (Two way ANOVA: $F_{(4, 20)} = 68.26$, p<0.001; post-hoc Bonferroni test: 1 μM vs. control at 48h or 72h: **p<0.001; 5 μM vs. control at 48 h or 72 h: **p<0.001; Fig. 2A). There is no difference between effect of 1 μM and 5 μM Aβ1-42 OCP on flash frequency (Two way ANOVA: $F_{(1, 20)} = 2.78$, p=0.11, Fig. 2A). Studies of the mechanism by which Aβ induces degeneration of neurons have suggested pivotal roles for increased levels of ROS (Goodman and Mattson, 1994; Bruce et al., 1996; Mark et al., 1997). As a measure of overall levels of oxidative stress in cultured NPCs, we quantified DCF fluorescence, an indicator of hydrogen peroxide levels. Prolonged exposure to Aβ1–42 OCP resulted in a progressive increase in DCF fluorescence (Two way ANOVA: $F_{(3, 24)} = 83.7$, p<0.001; Fig. 2C); exposure to 5 μM Aβ1–42 OCP resulted in a significant higher level of DCF fluorescence than 1 μM Aβ1–42 OCP (Two way ANOVA: $F_{(1, 24)} = 72.91$, p<0.001; Fig. 2C). Exposure to 1 μM Aβ1–42 OCP for up to 24 h did not significantly affect DCF fluorescence (post-hoc Bonferroni test: p=0.62), whereas a large elevation of DCF fluorescence occurred in NPC that had been exposed to 1 μM Aβ1–42 OCP for 48 or 72 hours (post-hoc Bonferroni test: 48 h: **p<0.001, 72 h: **p<0.001; Fig. 2B and 2C). Exposure to 5 μM Aβ1–42 OCP for up to 24 h resulted in a significant increase in DCF fluorescence, and a robust elevation of DCF fluorescence occurred in NPC that had been

exposed to Aβ1–42 OCP for 48 or 72 hours (post-hoc Bonferroni test: 24h: *p<0.05, 48h: **p<0.001, 72h: **p<0.001; Fig. 2B and 2C). Collectively, these findings indicate that SO flash activity diminishes as robust increase in global ROS occurs.

3.2. Mitochondrial dysfunction underlies the diminution of SO flash activity in NPCs during chronic exposure to Aβ1–42 OCP

Mitochondrial dysfunction plays an important role in the cascade of events by which aggregating Aβ induces degeneration of neurons (Keller et al., 1998; Bruce et al., 1996; Lustbader et al., 2004). Considering that SO flash activity requires electron transport chain function and is triggered by transient openings of mPTP (Wang et al., 2008; Hou et al., 2012), we hypothesized that the diminution in SO flash activity at 48 – 72 hours after exposure to Aβ1-42 OCP treatment might result from impaired mitochondrial function. We tested this possibility by monitoring mitochondrial membrane potential, cellular ATP levels and oxygen consumption at different time points during exposure of NPCs to Aβ1–42 OCP. Prolonged exposure to Aβ1–42 OCP resulted in a progressive decrease in mitochondrial membrane potential (Two way ANOVA: $F_{(2, 12)}$ =29.49, p<0.001). We found that fluorescence levels of the mitochondrial membrane potential-dependent fluorescent probe chloromethyl-X-rosamine (CMXRos) (Pendergrass et al., 2004) decreased by 15% and 26% within 24 hours of exposure to 1 μM and 5 μM Aβ1–42 OCP (post-hoc Bonferroni test: *p<0.05, Fig. 3B), respectively, and were markedly decreased by 30% or 42% at the 48 hour time point (post-hoc Bonferroni test: *p<0.05, **p<0.001, respectively, Fig. 3A and B). There is no significant difference between effect of 1 μM and 5 μM Aβ1–42 OCP on mitochondrial membrane potential (Two way ANOVA: $F_{(1, 12)}$ =3.09, p=0.10, Fig. 3B). Cellular ATP levels decreased progressively between 24 and 48 hours after exposure to Aβ1–42 OCP (Two way ANOVA: $F_{(3, 24)}$ =46.38, p<0.001, Fig. 3C), with 5 μM Aβ1–42 OCP causing a greater depletion of ATP compared to 1μM Aβ1–42 OCP (Two way ANOVA: $F_{(1, 24)}$ =7.71, p=0.01, Fig. 3C). Both 1 and 5μM Aβ1–42 OCP resulted in significant reduction in ATP level at 48 and 72 hours (post-hoc Bonferroni test: 48 and 72 hours: **p<0.001, Fig. 3C). Oxygen consumption decreased progressively between 24 and 48 hours after exposure to Aβ1–42 OCP (Two way ANOVA: $F_{(2, 12)}$ =9.89, p=0.002, Fig. 3D). Oxygen consumption was significantly reduced in NPCs that had been exposed to 5 μM Aβ1–42 OCP for 48 hours (post-hoc Bonferroni test: p<0.05), and there were trends towards reduced oxygen consumption in NPCs exposed to 1 or 5 μM Aβ1–42 OCP at 24 hours, and in NPCs exposed to 1 μM Aβ1–42 OCP for 48 hours (Fig. 3D). As expected, the oxygen consumption of NPCs was increased by the mitochondrial uncoupler FCCP and was decreased by oligomycin, an inhibitor of the ATP synthase (Supplemental Fig. 3), indicating that mitochondria are a major site of oxygen consumption in NPCs. Release of the mitochondrial intermembrane protein cytochrome c is an indicator of sustained mPTP opening and mitochondrial dysfunction (Rasola and Bernardi, 2007). We therefore evaluated cytochrome c subcellular localization at 24, 48 and 72 hours after exposure to Aβ1–42 OCP. Immunoblot analysis of cytochrome c levels in cytosolic and mitochondrial fractions revealed a significant increase in cytochrome c release from mitochondria in NPCs that had been exposed to 1 or 5 μM Aβ1–42 OCP for 48 or 72 hours (Two way ANOVA: $F_{(3, 16)}$ =33.94, p<0.001; post-hoc Bonferroni test: 48 or 72 hours: ** p<0.001; Fig. 3E and 3F), but not in NPCs exposed to Aβ1–42 OCP for 24 hours (post-hoc Bonferroni test: p=0.97, p=0.94, respectively, Fig. 3E and F). Double-label staining with a cytochrome c antibody and propidium iodide also indicated a reduction in mitochondrial cytochrome c levels accompanied by nuclear DNA condensation in many NPCs at 72 h after exposure to Aβ1–42 OCP (Supplemental Fig. 4). Collectively, these findings indicate decreased mitochondrial membrane potential and relatively preserved mitochondrial electron transport function contribute to the early increase in SO flash activity in NPCs exposed to Aβ1–42 OCP.

Subsequently, there is a collapse of mitochondrial membrane potential and deterioration of mitochondrial electron transport function which abolishes SO flash activity.

3.3. Aβ1–42 inhibits NPC proliferation by a mechanism involving the suppression of ERK signaling by mitochondrial SO

We previously reported that mitochondrial SO flashes negatively regulate the proliferation of NPCs by inhibiting extracellular signal-regulated kinase (ERK1/2) signaling under physiological conditions (Hou et al., 2012). We next asked whether exposure to Aβ1–42 OCP alters proliferation of NPCs. Treatment of neurospheres with Aβ OCP resulted in significant, concentration-dependent reductions in both the number of neurospheres formed and the diameter of individual neurospheres (One way ANOVA: $F_{(3, 8)} = 4.14$, $p=0.04$, Fig. 4A; $F_{(3, 8)} = 11.01$, $p=0.003$, Fig. 4B). 1 and 5 μM Aβ1-42 OCP exposure significantly decreased NS number and diameter (post-hoc Bonferroni test: *$p<0.05$, Fig. 4A; *$p<0.05$, **$p<0.001$, respectively, Fig. 4B). When adherent dissociated NPCs were exposed for 24 hours to 1 μM or 5 μM Aβ OCP, BrdU incorporation was significantly reduced by about 40% (post-hoc Bonferroni test: **$p<0.001$), Fig. 4C). In contrast, exposure to monomeric Aβ1–42 1 μM had no significant effect on BrdU incorporation (post-hoc Bonferroni test: $p=0.24$, Fig. 4C). To determine whether the Aβ-induced increase in mitochondrial SO production and suppression of cell proliferation were amenable to pharmacological intervention, we pretreated cultured NPCs with agents that specifically reduce SO flashes (Hou et al., 2012) or the global ROS scavenger N-acetyl-cysteine (NAC), and then exposed the cells to the 1 and 5 μM Aβ1-42 OCP for 24 h, and measured SO flashes and cell proliferation. MitoTEMPO, SS31, TMP, Tiron and CsA each significantly reduced SO flash incidence triggered by Aβ1–42 OCP (post-hoc Bonferroni test: **$p<0.001$, compared to NPCs treated with 1 μM or 5 μM Aβ1-42 OCP, Fig. 4D). All of the latter agents also significantly ameliorated the inhibitory effect of Aβ1-42 OCP on the proliferation of NPCs (post-hoc Bonferroni test: **$p<0.001$, compared to NPCs treated with 1 μM or 5 μM Aβ1-42 OCP, Fig. 4E). Treatment with NAC had no effect on SO flash incidence triggered by Aβ1–42 OCP, and did not modify the inhibition of NPCs caused by Aβ1–42 OCP (post-hoc Bonferroni test: 1 μM Aβ1-42 OCP +NAC vs. 1 μM Aβ1-42 OCP: $p=0.67$; 5 μM Aβ1-42 OCP +NAC vs. 5 μM Aβ1-42 OCP: $p=0.81$, Fig. 4D; 1 μM Aβ1-42 OCP +NAC vs. 1 μM Aβ1-42 OCP: $p=0.79$, 5 μM Aβ1-42 OCP +NAC vs. 5 μM Aβ1-42 OCP: $p=0.86$, Fig. 4E). Collectively, these findings suggest that mitochondrial SO flash activity mediates the adverse effects of aggregating Aβ on the self-renewal of NPCs.

We next examined the levels of phosphorylated ERK, JNK and p38 in NPCs exposed to Aβ1-42 OCP. To reduce the possible effect of global ROS on signaling pathways involved in regulating NPCs proliferation and survival, we chose 1 μM, not 5 μM, Aβ1-42 OCP because exposure of NPCs to 1 μM Aβ1-42 OCP caused a significant increase in SO flash incidence with little or no change of global ROS. Exposure of NPCs to 1 μM Aβ1–42 OCP for 24 h, a time point when SO flash activity was significantly elevated, resulted in significant reductions in the levels of activated ERKs 1 and 2 (p-ERK1 and p-ERK2) (post-hoc Bonferroni test: *$p<0.05$, Fig. 5A and B). Treatment of NPCs with mitoTEMPO, SS31, TMP, Tiron and CsA significantly attenuated the inhibitory effect of Aβ on ERK1 and ERK2 (post-hoc Bonferroni test: ** $p<0.05$, compared to NPCs treated with 1 μM Aβ1–42 OCP, Fig. 5A and B); in contrast, treatment of NPCs with NAC did not modify the Aβ1–42 OCP-induced reduction in phosphorylation of ERK1 and ERK2 (post-hoc Bonferroni test: p-ERK1: $p=0.87$; p-ERK2: $p=0.81$, Fig. 5A and B). Exposure of NPCs to 1 μM Aβ1–42 OCP for 24 h resulted in significant increases in the levels of active (phosphorylated) JNK2 and p38 (post-hoc Bonferroni test: *$p<0.05$, Fig. 5A and C). Treatment of NPCs with NAC, but not the agents that decreases SO flash incidence, significantly attenuated the activation of

JNK2 and p38 induced by exposure to 1 μM Aβ1–42 CP (post-hoc Bonferroni test: *p<0.05 Fig. 5A and C).

3.4. Elevation of global ROS and mitochondrial dysfunction mediate NPC death during chronic exposure to Aβ1–42 OCP

Sustained mitochondrial depolarization, ATP depletion and release of the intermembrane protein cytochrome c constitute a point of commitment to apoptotic cell death (Rasola and Bernardi, 2007). We next stained NPCs with the DNA-binding dye Hoechst 33258 and determined the percentage of cells exhibiting condensed and fragmented nuclear DNA typical of apoptotic death. Aβ1–42 OCP resulted in NPC death as exposure prolonged (Two way ANOVA: $F_{(3, 16)} =199.56$, $p<0.001$; Fig. 6A and B). Aβ1–42 OCP 1 and 5 μM induced NPC death in a concentration-dependent manner (Two way ANOVA: $F_{(1, 16)} =134.80$, $p<0.001$; Fig. 6A and B). We found Aβ1–42 OCP 1 and 5 μM caused significant NPC death at 48 and 72 h time points (post-hoc Bonferroni test: 48h: *p<0.0572h: **p<0.001 Fig. 6B), while no significant effect of Aβ1–42 OCP on cell death was observed at the 24 hour time point. Prolonged Aβ1–42 OCP exposure caused a significant release of LDH from NPCs (Two way ANOVA: $F_{(3, 16)} =541.87$, $p<0.001$, Fig. 6C). Consistently, 1 and 5 μM Aβ1–42 OCP caused a significant release of LDH from NPCs at the 48 and 72 h time points (post-hoc Bonferroni test: 48h: *p<0.05 72h: **p<0.001, Fig. 6C), and no significant increase in LDH release at the 24 hour time point (post-hoc Bonferroni test: p=0.07, p=0.06, respectively; Fig. 6C). 5 μM Aβ1–42 OCP resulted in more LDH release than 1 μM (Two way ANOVA: $F_{(1, 16)} =242.76$, $p<0.001$). Pretreatment of NPCs with TMP, Tiron and NAC before a 72 h-exposure to Aβ1–42 oligomers significantly reduced global ROS levels and LDH release (post-hoc Bonferroni test: *p<0.05, **p<0.001, Fig. 6D, 6E). Treatment of NPCs with NAC resulted in a more robust cytoprotective effect than TMP and Tiron. Treatment of NPCs with CsA did not affect global ROS levels, but decreased LDH levels (post-hoc Bonferroni test: p=0.55, Fig. 6D; p<0.001, Fig. 6E). Treatment of NPCs with MitoTEMPO and SS31 had no significant effects on either global ROS levels or LDH release in NPCs exposed to Aβ1-42 OCP (post-hoc Bonferroni test: p=0.59, p=0.86, respectively, Fig. 6D; p=0.32, p=0.46, respectively, Fig. 6E). Collectively, these findings demonstrate differential effects of mitochondrial SO flashes and global ROS on NPC death.

4. Discussion

There is considerable evidence, from studies of patients and experimental models, that brain cells are subjected to abnormally high levels of oxidative stress in AD. The involvement of ROS in AD pathogenesis has been inferred from the presence of oxidative modifications to proteins (carbonylation, nitration and covalent modification by 4-hydroxynonenal), lipids (lipid peroxidation products) and DNA (8-oxoguanine) (Mattson, 2004; Butterfield et al., 2011; Dumont et al., 2004; Gibson and Shi, 2010). We previously revealed a new paradigm of mitochondrial ROS production and signaling, namely, discontinuous, quantal bursts of SO which we termed flashes; SO flashes require transient opening of mPTPs under physiological conditions (Wang et al., 2008; Hou et al., 2012). In the present study we investigated the potential roles of mitochondrial SO flashes in regulating proliferation and survival in embryonic NPCs exposed to Aβ1–42 OCP. We demonstrated that an increase in SO flash activity is an early event in NPCs exposed to Aβ1–42 OCP and are essential for the inhibitory effect of Aβ1–42 on NPC proliferation. However, the delayed cell death that occurs in NPCs exposed to Aβ1–42 OCP is associated with a decrease in mitochondrial SO flashes, impaired mitochondrial function and a global increase in cellular oxidative stress.

4.1. SO flashes, initiated by transient mPTP opening, are early mitochondrial signals for inhibition of NPC proliferation by Aβ1-42 OCP

Amyloid β-peptide (Aβ) is implicated in the dysfunction and degeneration of neurons in AD, and can also inhibit neurogenesis. Long-term exposure of neurons to Aβ can cause mitochondrial oxidative damage, as indicated by mitochondrial depolarization, ATP depletion and release of cytochrome c and apoptosis (Keller et al., 1998; Hashimoto et al., 2003; Keil et al., 2004). In present study, we demonstrated that an increase in mitochondrial superoxide flash incidence is an early intracellular event caused by Aβ that inhibits NPC proliferation. It has been described previously that there are two gating modes of the classic mPTP: irreversible opening with high pore conductance; and transient opening with low pore conductance (Halestrap et al., 2009; Bernardi, 1999; Zoratti and Szabo, 1995; Petronilli et al., 1999; Hausenloy et al., 2004; Murphy and Steenbergen, 2008; Crompton et al., 1999). An increasing body of evidence indicates that the ignition of an SO flash is tightly coupled with transient opening of mPTPs (Wang et al., 2008; Ma et al., 2011). The Aβ-induced increase in SO flash frequency occurs within 6 hours of exposure and continues to increase through 24 h; the mPTP opening during this time period is assumed to be transient because no cytochrome c is released from the mitochondria. However, this early period of transient mPTP opening and SO production is followed by a pathological sustained opening of the mPTP which is associated with mitochondrial membrane depolarization, cessation of mitochondrial SO flashes and a sustained increase in global cellular ROS levels. At 48 and 72 h after exposure to Aβ1-42 OCP, the SO flashes were greatly diminished or absent and considerable cytochrome c was released from the mitochondria, consistent with sustained mPTP opening. The cessation of SO flash activity accompanied by a robust elevation of global ROS from 48 to 72 h is likely the result of a combination of membrane-associated oxidative stress and mitochondrial functional impairment (Butterfield et al., 2011; Begley et al., 1999; Mark et al., 1995). More direct effects of Aβ on mitochondria have also been described including impairment of electron transport and inhibition of Mn-SOD (Caspersen et al., 2005; Anantharaman et al., 2006). Our findings indicate that there is a switch from early transient mPTP opening and SO flashes, to the later irreversible mPTP opening and sustained SO generation during the time course of exposure of NPCs to Aβ (Figure 7). The later events support the notion that mitochondrial oxidative damage leads to irreversible mPTP opening and reduced ATP synthesis. We have thus discovered that SO flashes are an early mitochondrial response to Aβ, which was previously unknown and may therefore be a target for therapeutic interventions in the future.

4.2. Differential regulation of NPC proliferation and death by mitochondrial SO flashes and global cellular ROS

Neurogenesis, the production of new neurons from neural progenitor cells (NPCs), occurs during whole embryonic brain developmental processes and in restricted regions of the adult brain. Exposure of NPCs to Aβ in cell culture and in vivo has been shown to adversely affect one or more processes involved in adult neurogenesis including cell proliferation, differentiation and survival (Haughey et al., 2002; Donovan et al., 2006; Zhang et al., 2007; Ermini et al., 2008; Rodriguez et al., 2008; Shruster et al., 2010). Sustained irreversible, full conductance mPTP opening is a pivotal event in apoptosis (Petronilli et al., 1999; Green et al., 2004; Martinou et al., 2001; Bernardi et al., 2007) and is implicated in the death of neurons that occurs in AD (Cotman and Su, 1996; Guo et al., 1997; Mattson, 2008). However, the function of mPTPs in physiological settings is poorly understood, and the mechanism of coupling of mPTP to the electron transport chain complexes that generate SO is unknown. Using primary embryonic cortical NPC cultures, we found that exposure of NPCs to an Aβ OCP results in increased SO flash production during a 6 – 24 h period that requires mPTP opening and a functional electron transport chain. Both mPTP opening and SO flashes were necessary for the inhibition of NPC proliferation by Aβ OCP because

cyclosporine A (mPTP inhibitor) and Tiron, mito-TEMPO, TMP and SS1 (inhibitors or scavengers of SO) prevented the inhibition of cell proliferation in NPC exposed to Aβ OCP. The mechanism by which Aβ OCP inhibit NPC proliferation involves inhibition of ERKs which are kinases previously shown to promote NPC proliferation (Cheng et al., 2004; Zhou and Miller, 2006; Samuels et al., 2008).

Extended exposure to Aβ OCP over a period of several days caused significant NPC death, which was significantly attenuated by blocking global ROS with NAC, whereas specific SO flash blockers (mitoTEMP and SS31) were less effective (Fig. 6D and E). These results indicate that early quantal SO production and late pan-cellular oxidative stress have different roles in the adverse effects of Aβ OCP on NPCs; early SO flashes inhibit cell proliferation, whereas delayed cell death involves uncontrolled global oxidative stress. Differentiation of embryonic NPC into neurons is associated with increased mitochondrial SO flash generation and selectively blocking the flashes enhances proliferation and inhibits differentiation (Hou et al., 2012). Previous cell culture studies have provided evidence that Aβ can directly inhibit the proliferation of NPCs (Haughey et al., 2002a, 2002b; Mazur-Kolecka et al., 2006). On the other hand, studies of APP mutant and APP/PS1 double-mutant mice have provided seemingly conflicting results with some investigators reporting reduced (Haughey et al. 2002a, 2002b; Donovan et al., 2006; Verret et al., 2007; Rodriguez et al., 2008; Crews et al., 2010; Hamilton et al., 2010; Faure et al., 2011), and others increased (Jin et al., 2004; Gan et al., 2008; Sotthibundhu et al., 2009), NPC proliferation. However, the interpretation of the results of studies of APP, PS1 and APP/PS1 double-mutant transgenic mice are complicated by evidence that full-length APP, secreted forms of APP and C-terminal APP fragments can alter neurogenesis (Kwak et al., 2006), and that PS1 exerts APP-independent actions including cleavage of Notch, a well-known regulator of NPC fate (Wen et al., 2004). Nevertheless, we cannot rule out the possibility that the mPTP-mediated superoxide flash-based mechanism by which Aβ inhibited the proliferation of embryonic cortical NPCs in the present study may not occur in NPCs in the adult brain. However, the available data suggest that the signaling mechanisms that regulate the self-renewal and differentiation of adult NPCs are very similar, if not identical, to those that regulate embryonic NPCs (Lathia et a., 2007).

Analyses of adult NPC proliferation and neurogenesis in APP mutant mice suggest that subtoxic levels of Aβ can inhibit adult NPC proliferation while enhancing their differentiation into neurons (Gan et al., 2008). Others have found that the survival of newly-generated neurons is reduced in the hippocampus of transgenic mice with Aβ deposits in the dentate gyrus (Verret et al., 2007), consistent with evidence that newly-generated neurons are particularly prone to apoptosis (Cheng et al., 2007). Altogether, the available data suggest that low levels of Aβ can reduce adult NPC proliferation and promote neuronal differentiation which might be an adaptive response in the early stages of AD pathogenesis. However, chronic accumulation of Aβ results in the death of both newly-generated and mature neurons, and associated cognitive impairment.

4.3. Mitochondrial SO flash production and MAP kinase signaling

Levels of activated (phosphorylated) ERKs 1 and 2 were suppressed early (within the first 24 h) during exposure to Aβ1-42 OCP whereas p38 and JNK were activated in response to Aβ1-42 OCP. Previous studies have demonstrated roles for ERKs 1 and 2 in promoting the survival of NPCs (Zhao et al., 2007) and protecting neurons against Aβ toxicity (Jin et al., 2005). On the other hand, increased ROS levels often result in the activation of p38 and JNK (Finkel and Holbrook, 2000; Gotoh and Cooper, 1998; Essers, et al., 2004; Owusu-Ansah and Banerjee, 2009), two kinases involved in oxidative stress-induced death of NPCs (Cheng et al., 2001) and Aβ-induced death of neurons (Jin et al., 2005; Tamagno et al., 2003). We found that exposure of NPCs to 1 μM Aβ1-42 OCPs for 24 h resulted in

significant reductions (~30%) in the levels of p-ERK1 and p-ERK2 and more modest (~10%) inhibition of p-p38 and p-JNK. Here we treated the NPC with 1 μM Aβ1-42 OCPs, which caused significant increases in flash activity, but little change of global ROS within 24h treatments. During the first 24 hours of exposure to1 μM Aβ1-42 OCP we observed little or no change of p-JNK or p-p38 levels, consistent with the latter kinases not being activated by mitochondrial SO flashes. We found that treatment of NPCs with agents that reduced mitochondrial SO flash activity significantly attenuated the inhibitory effect of Aβ on phosphorylation of ERK1 and ERK2, but did not prevent the delayed activation of JNK2 and P38 associated with a global increase in cellular ROS. In contrast, treatment of NPCs with NAC did not modify the reduction in phosphorylation of ERK1 and ERK2, but did reduce activation of JNK2 and P38. Our findings therefore suggest a role for mitochondrial SO production in the inhibition of ERKs 1/2 and consequent reduction in NPC proliferation, and a role for global ROS in activation of JNK that mediates Aβ-induced cell death. Collectively, our findings show that increased SO flash activity and decreased ERK activation underlies the inhibition of NPC proliferation by Aβ1-42 OCPs.

In summary, we provide evidence for several previously unknown roles for bursts of mitochondrial SO production in NPCs pathophysiology. In the pathological setting of exposure to aggregating Aβ1–42, which is believed to play a pivotal role in the pathogenesis of AD, there initially occurs a significant elevation of mitochondrial SO flash activity during the first 24 hours which inhibits NPC proliferation (Fig. 7). Subsequently, there was a global ROS elevation and sustained opening of mPTP and electron transport chain dysfunction, associated with disappearance of mitochondrial SO flashes, and resulting in NPC death. We first demonstrated the switch from transient to irreversible mPTP opening and increased quantal SO flashes activity is a very early mitochondrial signal before the global ROS elevation and mitochondrial oxidative damages during the time course of Aβ treatments. Moreover, the early increased SO flashes negatively regulate NPC proliferation suggests a novel mechanism for impaired neurogenesis by Aβ. Previous studies have shown that environmental enrichment, exercise and dietary energy restriction can promote neurogenesis in normal adult rodents (van Praag et al., 1999; Kempermann et al., 2002; Lee et al., 2002) and can protect against adverse cellular effects of Aβ and cognitive impairment in mouse models of AD (Halagappa et al., 2007; Parachikova et al., 2008; Mirochnic et al., 2009). It will be of considerable interest to determine whether the mechanism by which such factors that affect neurogenesis involves changes in mitochondrial SO flash-mediated signaling.

Supplementary Material

Refer to Web version on PubMed Central for supplementary material.

Acknowledgments

References

Anantharaman M, Tangpong J, Keller JN, Murphy MP, Markesbery WR, Kiningham KK, St Clair DK. Beta-amyloid mediated nitration of manganese superoxide dismutase: implication for oxidative stress in an APPNLH/NLH X PS-1P264L/P264L double knock-in mouse model of Alzheimer's disease. Am J Pathol. 2006; 168:1608–1618. [PubMed: 16651627]

Begley JG, Duan W, Chan S, Duff K, Mattson MP. Altered calcium homeostasis and mitochondrial dysfunction in cortical synaptic compartments of presenilin-1 mutant mice. J Neurochem. 1999; 72:1030–1039. [PubMed: 10037474]

Bernardi P. Mitochondrial transport of cations: channels, exchangers, and permeability transition. Physiol Rev. 1999; 79:1127–1155. [PubMed: 10508231]

Bernardi P, Forte M. The mitochondrial permeability transition pore. Novartis Found Symp. 2007; 287:157–164. [PubMed: 18074637]

Bizon JL, Lee HJ, Gallagher M. Neurogenesis in a rat model of age-related cognitive decline. Aging Cell. 2004; 3:227–234. [PubMed: 15268756]

Bonda DJ, Wang X, Perry G, Nunomura A, Tabaton M, Zhu X, Smith MA. Oxidative stress in Alzheimer disease: a possibility for prevention. Neuropharmacology. 2010; 59:290–294. [PubMed: 20394761]

Bruce AJ, Malfroy B, Baudry M. beta-Amyloid toxicity in organotypic hippocampal cultures: protection by EUK-8, a synthetic catalytic free radical scavenger. Proc Natl Acad Sci U S A. 1996; 93:2312–2316. [PubMed: 8637869]

Butterfield DA, Reed T, Sultana R. Roles of 3-nitrotyrosine- and 4-hydroxynonenal-modified brain proteins in the progression and pathogenesis of Alzheimer's disease. Free Radic Res. 2011; 45:59–72. [PubMed: 20942567]

Caspersen C, Wang N, Yao J, Sosunov A, Chen X, Lustbader JW, Xu HW, Stern D, McKhann G, Yan SD. Mitochondrial Abeta: a potential focal point for neuronal metabolic dysfunction in Alzheimer's disease. FASEB J. 2005; 19:2040–1. [PubMed: 16210396]

Cheng A, Chan SL, Milhavet O, Wang S, Mattson MP. p38 MAP kinase mediates nitric oxide-induced apoptosis of neural progenitor cells. J Biol Chem. 2001; 276:43320–43327. [PubMed: 11555660]

Cheng A, Tang H, Cai J, Zhu M, Zhang X, Rao M, Mattson MP. Gap junctional communication is required to maintain mouse cortical neural progenitor cells in a proliferative state. Dev Biol. 2004; 272:203–216. [PubMed: 15242801]

Cheng A, Shin-ya K, Wan R, Tang SC, Miura T, Tang H, Khatri R, Gleichman M, Ouyang X, Liu D, Park HR, Chiang JY, Mattson MP. Telomere protection mechanisms change during neurogenesis and neuronal maturation: newly generated neurons are hypersensitive to telomere and DNA damage. J Neurosci. 2007; 27:3722–3733. [PubMed: 17409236]

Cheng A, Coksaygan T, Tang H, Khatri R, Balice-Gordon RJ, Rao MS, Mattson MP. Truncated tyrosine kinase B brain-derived neurotrophic factor receptor directs cortical neural stem cells to a glial cell fate by a novel signaling mechanism. J Neurochem. 2007; 100:1515–1530. [PubMed: 17286628]

Cho S, Szeto HH, Kim E, Kim H, Tolhurst AT, Pinto JT. A novel cell-permeable antioxidant peptide, SS31, attenuates ischemic brain injury by down-regulating CD36. J Biol Chem. 2007; 282:4634–4642. [PubMed: 17178711]

Cotman CW, Su JH. Mechanisms of neuronal death in Alzheimer's disease. Brain Pathol. 1996; 6:493–506. [PubMed: 8944319]

Crews L, Adame A, Patrick C, Delaney A, Pham E, Rockenstein E, Hansen L, Masliah E. Increased BMP6 levels in the brains of Alzheimer's disease patients and APP transgenic mice are accompanied by impaired neurogenesis. J Neurosci. 2010; 30:12252–12262. [PubMed: 20844121]

Crompton M, Virji S, Doyle V, Johnson N, Ward JM. The mitochondrial permeability transition pore. Biochem Soc Symp. 1999; 66:167–179. [PubMed: 10989666]

Demars M, Hu YS, Gadadhar A, Lazarov O. Impaired neurogenesis is an early event in the etiology of familial Alzheimer's disease in transgenic mice. J Neurosci Res. 2010; 88:2103–2117. [PubMed: 20209626]

Donovan MH, Yazdani U, Norris RD, Games D, German DC, Eisch AJ. Decreased adult hippocampal neurogenesis in the PDAPP mouse model of Alzheimer's disease. J Comp Neurol. 2006; 495:70–83. [PubMed: 16432899]

Dumont M, Lin MT, Beal MF. Mitochondria and antioxidant targeted therapeutic strategies for Alzheimer's disease. J Alzheimers Dis. 2010; 20:S633–643. [PubMed: 20421689]

Dupret D, Revest JM, Koehl M, Ichas F, De Giorgi F, Costet P, Abrous DN, Piazza PV. Spatial relational memory requires hippocampal adult neurogenesis. PLoS One. 2008; 3:e1959. [PubMed: 18509506]

Ermini FV, Grathwohl S, Radde R, Yamaguchi M, Staufenbiel M, Palmer TD, Jucker M. Neurogenesis and alterations of neural stem cells in mouse models of cerebral amyloidosis. Am J Pathol. 2008; 172:1520–1528. [PubMed: 18467698]

Esposito L, Raber J, Kekonius L, Yan F, Yu GQ, Bien-Ly N, Puoliväli J, Scearce-Levie K, Masliah E, Mucke L. Reduction in mitochondrial superoxide dismutase modulates Alzheimer's disease-like pathology and accelerates the onset of behavioral changes in human amyloid precursor protein transgenic mice. J Neurosci. 2006; 26:5167–5179. [PubMed: 16687508]

Essers MA, Weijzen S, de Vries-Smits AM, Saarloos I, de Ruiter ND, Bos JL, Burgering BM. FOXO transcription factor activation by oxidative stress mediated by the small GTPase Ral and JNK. EMBO J. 2004; 23:4802–4812. [PubMed: 15538382]

Faure A, Verret L, Bozon B, El Tannir El Tayara N, Ly M, Kober F, Dhenain M, Rampon C, Delatour B. Impaired neurogenesis, neuronal loss, and brain functional deficits in the APPxPS1-Ki mouse model of Alzheimer's disease. Neurobiol Aging. 2011; 32:407–418. [PubMed: 19398247]

Finkel T, Holbrook NJ. Oxidants, oxidative stress and the biology of ageing. Nature. 2000; 408:239–247. [PubMed: 11089981]

Gabuzda D, Busciglio J, Chen LB, Matsudaira P, Yankner BA. Inhibition of energy metabolism alters the processing of amyloid precursor protein and induces a potentially amyloidogenic derivative. J Biol Chem. 1994; 269:13623–13628. [PubMed: 8175797]

Gan L, Qiao S, Lan X, Chi L, Luo C, Lien L, Yan Liu Q, Liu R. Neurogenic responses to amyloid-beta plaques in the brain of Alzheimer's disease-like transgenic (pPDGF-APPSw,Ind) mice. Neurobiol Dis. 2008; 29:71–80. [PubMed: 17916429]

Gibson GE, Shi Q. A mitocentric view of Alzheimer's disease suggests multi-faceted treatments. J Alzheimers Dis. 2010; 20:S591–607. [PubMed: 20463407]

Goedert M, Spillantini MG. A century of Alzheimer's disease. Science. 2006; 314:777–81. [PubMed: 17082447]

Goodman Y, Mattson MP. Secreted forms of beta-amyloid precursor protein protect hippocampal neurons against amyloid beta-peptide-induced oxidative injury. Exp Neurol. 1994; 128:1–12. [PubMed: 8070512]

Gotoh Y, Cooper JA. Reactive oxygen species- and dimerization-induced activation of apoptosis signal-regulating kinase 1 in tumor necrosis factor-alpha signal transduction. J Biol Chem. 1998; 273:17477–17482. [PubMed: 9651337]

Green DR, Kroemer G. The pathophysiology of mitochondrial cell death. Science. 2004; 305:626–629. [PubMed: 15286356]

Guo Q, Sopher BL, Furukawa K, Pham DG, Robinson N, Martin GM, Mattson MP. Alzheimer's presenilin mutation sensitizes neural cells to apoptosis induced by trophic factor withdrawal and amyloid beta-peptide: involvement of calcium and oxyradicals. J Neurosci. 1997; 17:4212–4222. [PubMed: 9151738]

Gwon AR, Park JS, Arumugam TV, Kwon YK, Chan SL, Kim SH, Baik SH, Yang S, Yun YK, Choi Y, Kim S, Tang SC, Hyun DH, Cheng A, Dann CE 3rd, Bernier M, Lee J, Markesbery WR, Mattson MP, Jo DG. Oxidative lipid modification of nicastrin enhances amyloidogenic-secretase activity in Alzheimer's disease. Aging Cell. 2012; 11:559–568. [PubMed: 22404891]

Halagappa VK, Guo Z, Pearson M, Matsuoka Y, Cutler RG, Laferla FM, Mattson MP. Intermittent fasting and caloric restriction ameliorate age-related behavioral deficits in the triple-transgenic mouse model of Alzheimer's disease. Neurobiol Dis. 2007; 26:212–220. [PubMed: 17306982]

Halestrap AP. What is the mitochondrial permeability transition pore? J Mol Cell Cardiol. 2009; 46:821–831. [PubMed: 19265700]

Hamilton LK, Aumont A, Julien C, Vadnais A, Calon F, Fernandes KJ. Widespread deficits in adult neurogenesis precede plaque and tangle formation in the 3xTg mouse model of Alzheimer's disease. Eur J Neurosci. 2010; 32(6):905–20. [PubMed: 20726889]

Hardy J. A hundred years of Alzheimer's disease research. Neuron. 2006; 52:3–13. [PubMed: 17015223]

Hashimoto T, Elder CM, Okun MS, Patrick SK, Vitek JL. Stimulation of the subthalamic nucleus changes the firing pattern of pallidal neurons. J Neurosci. 2003; 23:1916–23. [PubMed: 12629196]

Haughey NJ, Nath A, Chan SL, Borchard AC, Rao MS, Mattson MP. Disruption of neurogenesis by amyloid beta-peptide, and perturbed neural progenitor cell homeostasis, in models of Alzheimer's disease. J Neurochem. 2002a; 83:1509–24. [PubMed: 12472904]

Haughey NJ, Liu D, Nath A, Borchard AC, Mattson MP. Disruption of neurogenesis in the subventricular zone of adult mice, and in human cortical neuronal precursor cells in culture, by amyloid beta-peptide: implications for the pathogenesis of Alzheimer's disease. Neuromolecular Med. 2002b; 1:125–135. [PubMed: 12025858]

Hausenloy D, Wynne A, Duchen M, Yellon D. Transient mitochondrial permeability transition pore opening mediates preconditioning-induced protection. Circulation. 2004; 109:1714–1717. [PubMed: 15066952]

Hensley K, Carney JM, Mattson MP, Aksenova M, Harris M, Wu JF, Floyd RA, Butterfield DA. A model for beta-amyloid aggregation and neurotoxicity based on free radical generation by the peptide: relevance to Alzheimer disease. Proc Natl Acad Sci U S A. 1994; 91:3270–3274. [PubMed: 8159737]

Hou Y, Ouyang X, Wan R, Cheng H, Mattson MP, Cheng A. Mitochondrial superoxide production negatively regulates neural progenitor proliferation and cerebral cortical development. Stem Cells. 2012; 30:2535–2547. [PubMed: 22949407]

Huang X, Atwood CS, Hartshorn MA, Multhaup G, Goldstein LE, Scarpa RC, Cuajungco MP, Gray DN, Lim J, Moir RD, Tanzi RE, Bush AI. The A beta peptide of Alzheimer's disease directly produces hydrogen peroxide through metal ion reduction. Biochemistry. 1999; 38:7609–7616. [PubMed: 10386999]

Jin Y, Yan EZ, Fan Y, Zong ZH, Qi ZM, Li Z. Sodium ferulate prevents amyloid-beta-induced neurotoxicity through suppression of p38 MAPK and upregulation of ERK-1/2 and Akt/protein kinase B in rat hippocampus. Acta Pharmacol Sin. 2005; 26:943–951. [PubMed: 16038626]

Jin K, Galvan V, Xie L, Mao XO, Gorostiza OF, Bredesen DE, Greenberg DA. Enhanced neurogenesis in Alzheimer's disease transgenic (PDGF-APPSw,Ind) mice. Proc Natl Acad Sci U S A. 2004; 101:13363–13367. [PubMed: 15340159]

Jo DG, Arumugam TV, Woo HN, Park JS, Tang SC, Mughal M, Hyun DH, Park JH, Choi YH, Gwon AR, Camandola S, Cheng A, Cai H, Song W, Markesbery WR, Mattson MP. Evidence that gamma-secretase mediates oxidative stress-induced beta-secretase expression in Alzheimer's disease. Neurobiol Aging. 2010; 31:917–925. [PubMed: 18687504]

Keil U, Bonert A, Marques CA, Scherping I, Weyermann J, Strosznajder JB, Müller-Spahn F, Haass C, Czech C, Pradier L, Müller WE, Eckert A. Amyloid beta-induced changes in nitric oxide production and mitochondrial activity lead to apoptosis. J Biol Chem. 2004; 279:50310–50320. [PubMed: 15371443]

Keller JN, Kindy MS, Holtsberg FW, St Clair DK, Yen HC, Germeyer A, Steiner SM, Bruce-Keller AJ, Hutchins JB, Mattson MP. Mitochondrial manganese superoxide dismutase prevents neural apoptosis and reduces ischemic brain injury: suppression of peroxynitrite production, lipid peroxidation, and mitochondrial dysfunction. J Neurosci. 1998; 18:687–697. [PubMed: 9425011]

Kempermann G, Gast D, Gage FH. Neuroplasticity in old age: sustained fivefold induction of hippocampal neurogenesis by long-term environmental enrichment. Ann Neurol. 2002; 52:135–143. [PubMed: 12210782]

Klein WL, Krafft GA, Finch CE. Targeting small Aβ oligomers: the solution to an Alzheimer's disease conundrum? Trends Neurosci. 2001; 24:219–224. [PubMed: 11250006]

Kwak YD, Brannen CL, Qu T, Kim HM, Dong X, Soba P, Majumdar A, Kaplan A, Beyreuther K, Sugaya K. Amyloid precursor protein regulates differentiation of human neural stem cells. Stem Cells Dev. 2006; 15:381–389. [PubMed: 16846375]

Lathia JD, Rao MS, Mattson MP, Ffrench-Constant C. The microenvironment of the embryonic neural stem cell: lessons from adult niches? Dev Dyn. 2007; 236:3267–82. [PubMed: 17937403]

Lathia JD, Okun E, Tang SC, Griffioen K, Cheng A, Mughal MR, Laryea G, Selvaraj PK, ffrench-Constant C, Magnus T, Arumugam TV, Mattson MP. Toll-like receptor 3 is a negative regulator of embryonic neural progenitor cell proliferation. J Neurosci. 2008; 28:13978–13984. [PubMed: 19091986]

Lazarov O, Mattson MP, Peterson DA, Pimplikar SW, van Praag H. When neurogenesis encounters aging and disease. Trends Neurosci. 2010; 33:569–579. [PubMed: 20961627]

Lee J, Duan W, Mattson MP. Evidence that brain-derived neurotrophic factor is required for basal neurogenesis and mediates, in part, the enhancement of neurogenesis by dietary restriction in the hippocampus of adult mice. J Neurochem. 2002; 82:1367–1375. [PubMed: 12354284]

Lustbader JW, Cirilli M, Lin C, Xu HW, Takuma K, Wang N, Caspersen C, Chen X, Pollak S, Chaney M, Trinchese F, Liu S, Gunn-Moore F, Lue LF, Walker DG, Kuppusamy P, Zewier ZL, Arancio O, Stern D, Yan SS, Wu H. ABAD directly links Abeta to mitochondrial toxicity in Alzheimer's disease. Science. 2004; 304:448–452. [PubMed: 15087549]

Ma DK, Kim WR, Ming GL, Song H. Activity-dependent extrinsic regulation of adult olfactory bulb and hippocampal neurogenesis. Ann N Y Acad Sci. 2009; 1170:664–673. [PubMed: 19686209]

Mark RJ, Hensley K, Butterfield DA, Mattson MP. Amyloid beta-peptide impairs ion-motive ATPase activities: evidence for a role in loss of neuronal Ca2+ homeostasis and cell death. J Neurosci. 1995; 15:6239–6249. [PubMed: 7666206]

Mark RJ, Pang Z, Geddes JW, Uchida K, Mattson MP. Amyloid beta-peptide impairs glucose transport in hippocampal and cortical neurons: involvement of membrane lipid peroxidation. J Neurosci. 1997; 17:1046–1054. [PubMed: 8994059]

Martinou JC, Green DR. Breaking the mitochondrial barrier. Nat Rev Mol Cell Biol. 2001; 2:63–67. [PubMed: 11413467]

Mattson MP. Pathways towards and away from Alzheimer's disease. Nature. 2004; 430:631–639. [PubMed: 15295589]

Mattson MP, Gleichmann M, Cheng A. Mitochondria in neuroplasticity and neurological disorders. Neuron. 2008; 60:748–766. [PubMed: 19081372]

Mazur-Kolecka B, Golabek A, Nowicki K, Flory M, Frackowiak J. Amyloid-beta impairs development of neuronal progenitor cells by oxidative mechanisms. Neurobiol Aging. 2006; 27:1181–1192. [PubMed: 16105709]

Mirochnic S, Wolf S, Staufenbiel M, Kempermann G. Age effects on the regulation of adult hippocampal neurogenesis by physical activity and environmental enrichment in the APP23 mouse model of Alzheimer disease. Hippocampus. 2009; 19:1008–1018. [PubMed: 19219917]

Murphy E, Steenbergen C. Mechanisms underlying acute protection from cardiac ischemia-reperfusion injury. Physiol Rev. 2008; 88:581–609. [PubMed: 18391174]

Owusu-Ansah E, Banerjee U. Reactive oxygen species prime Drosophila haematopoietic progenitors for differentiation. Nature. 2009; 461:537–541. [PubMed: 19727075]

Parachikova A, Nichol KE, Cotman CW. Short-term exercise in aged Tg2576 mice alters neuroinflammation and improves cognition. Neurobiol Dis. 2008; 30:121–129. [PubMed: 18258444]

Pendergrass W, Wolf N, Poot M. Efficacy of MitoTracker Green and CMXrosamine to measure changes in mitochondrial membrane potentials in living cells and tissues. Cytometry A. 2004; 61:162–169. [PubMed: 15382028]

Petronilli V, Miotto G, Canton M, Brini M, Colonna R, Bernardi P, Di Lisa F. Transient and long-lasting openings of the mitochondrial permeability transition pore can be monitored directly in intact cells by changes in mitochondrial calcein fluorescence. Biophys J. 1999; 76:725–734. [PubMed: 9929477]

Rasola A, Bernardi P. The mitochondrial permeability transition pore and its involvement in cell death and in disease pathogenesis. Apoptosis. 2007; 12:815–833. [PubMed: 17294078]

Rodríguez JJ, Jones VC, Tabuchi M, Allan SM, Knight EM, LaFerla FM, Oddo S, Verkhratsky A. Impaired adult neurogenesis in the dentate gyrus of a triple transgenic mouse model of Alzheimer's disease. PLoS One. 2008; 3:e2935. [PubMed: 18698410]

Samuels IS, Karlo JC, Faruzzi AN, Pickering K, Herrup K, Sweatt JD, Saitta SC, Landreth GE. Deletion of ERK2 mitogen-activated protein kinase identifies its key roles in cortical neurogenesis and cognitive function. J Neurosci. 2008; 28:6983–6995. [PubMed: 18596172]

Schieke SM, Phillips D, McCoy JP Jr, Aponte AM, Shen RF, Balaban RS, Finkel T. The mammalian target of rapamycin (mTOR) pathway regulates mitochondrial oxygen consumption and oxidative capacity. J Biol Chem. 2006; 281:27643–27652. [PubMed: 16847060]

Shankar GM, Bloodgood BL, Townsend M, Walsh DM, Selkoe DJ, Sabatini BL. Natural oligomers of the Alzheimer amyloid-beta protein induce reversible synapse loss by modulating an NMDA-type glutamate receptor-dependent signaling pathway. J Neurosci. 2007; 27:2866–2875. [PubMed: 17360908]

Shruster A, Eldar-Finkelman H, Melamed E, Offen D. Wnt signaling pathway overcomes the disruption of neuronal differentiation of neural progenitor cells induced by oligomeric amyloid β-peptide. J Neurochem. 2010; 116:522–529. [PubMed: 21138436]

Sotthibundhu A, Li QX, Thangnipon W, Coulson EJ. Abeta(1–42) stimulates adult SVZ neurogenesis through the p75 neurotrophin receptor. Neurobiol Aging. 2009; 30:1975–1985. [PubMed: 18374455]

Tamagno E, Robino G, Obbili A, Bardini P, Aragno M, Parola M, Danni O. H2O2 and 4-hydroxynonenal mediate amyloid beta-induced neuronal apoptosis by activating JNKs and p38MAPK. Exp Neurol. 2003; 180:144–155. [PubMed: 12684028]

Tamagno E, Guglielmotto M, Aragno M, Borghi R, Autelli R, Giliberto L, Muraca G, Danni O, Zhu X, Smith MA, Perry G, Jo DG, Mattson MP, Tabaton M. Oxidative stress activates a positive feedback between the gamma- and beta-secretase cleavages of the beta-amyloid precursor protein. J Neurochem. 2008; 104:683–695. [PubMed: 18005001]

van Praag H, Kempermann G, Gage FH. Running increases cell proliferation and neurogenesis in the adult mouse dentate gyrus. Nat Neurosci. 1999; 2:266–270. [PubMed: 10195220]

Verret L, Jankowsky JL, Xu GM, Borchelt DR, Rampon C. Alzheimer's-type amyloidosis in transgenic mice impairs survival of newborn neurons derived from adult hippocampal neurogenesis. J Neurosci. 2007; 27:6771–6780. [PubMed: 17581964]

Wang W, Fang H, Groom L, Cheng A, Zhang W, Liu J, Wang X, Li K, Han P, Zheng M, Yin J, Wang W, Mattson MP, Kao JP, Lakatta EG, Sheu SS, Ouyang K, Chen J, Dirksen RT, Cheng H. Superoxide flashes in single mitochondria. Cell. 2008; 134:279–290. [PubMed: 18662543]

Wen PH, Hof PR, Chen X, Gluck K, Austin G, Younkin SG, Younkin LH, DeGasperi R, Gama Sosa MA, Robakis NK, Haroutunian V, Elder GA. The presenilin-1 familial Alzheimer disease mutant P117L impairs neurogenesis in the hippocampus of adult mice. Exp Neurol. 2004; 188:224–237. [PubMed: 15246822]

Zhang C, McNeil E, Dressler L, Siman R. Long-lasting impairment in hippocampal neurogenesis associated with amyloid deposition in a knock-in mouse model of familial Alzheimer's disease. Exp Neurol. 2007; 204:77–87. [PubMed: 17070803]

Zhao Y, Xiao Z, Gao Y, Chen B, Zhao Y, Zhang J, Dai J. Insulin rescues ES cell-derived neural progenitor cells from apoptosis by differential regulation of Akt and ERK pathways. Neurosci Lett. 2007; 429:49–45. [PubMed: 17980966]

Zhou L, Miller CA. Mitogen-activated protein kinase signaling, oxygen sensors and hypoxic induction of neurogenesis. Neurodegener Dis. 2006; 3:50–55. [PubMed: 16909037]

Zoratti M, Szabo I. The mitochondrial permeability transition. Biochim Biophys Acta. 1995; 1241:139–176. [PubMed: 7640294]
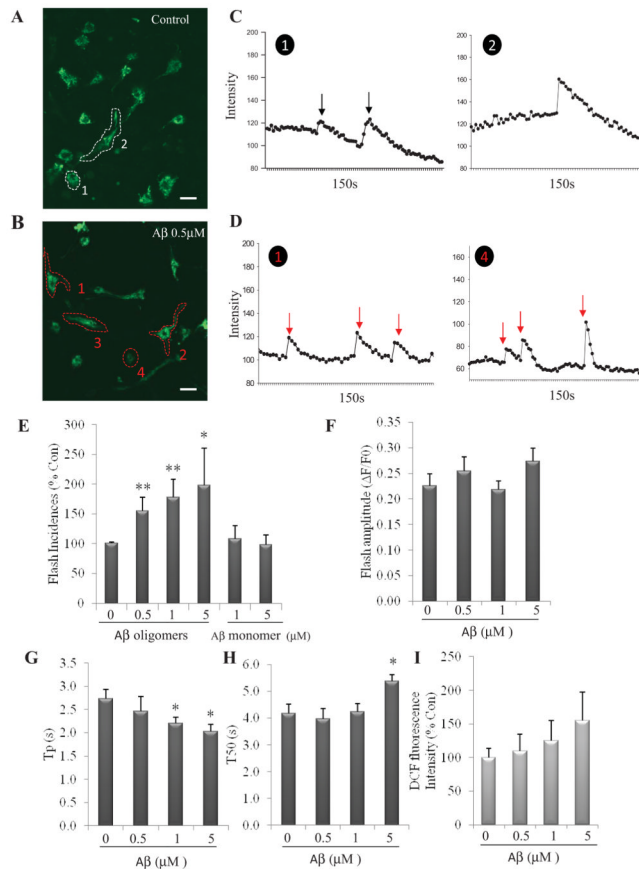
Figure 1. An Aβ1-42 oligomer-containing preparation induces an early increase in mitochondrial SO flash incidence in NPCs

(**A and B**) Confocal images of mitochondrial SO in NPCs expressing mt-cpYFP that had been treated for 24 h with either vehicle control (A) or 0.5 µM Aβ1-42 OCP (B). Two supplemental videos showing mitochondrial SO flashes in NPCs that cover a 3 minute imaging period can be viewed online. The circled/numbered NPCs in panels A and B (cells n 1 and 2 cells in panel A and cells 1, 2, 3, 4 cells in B) exhibited a mitochondrial SO flash during the video recording period. Bar = 10 µm. (**C and D**) Sample recordings of mt-cpYFP fluorescence in NPCs that had been treated for 24 h with either vehicle control (C, cells 1 and 2 in panel A) or 0.5 µM Aβ1-42 OCP (D, cells 1 and 4 cells in panel B). Each arrow shows a SO flash. (**E**) SO flash incidence (percentage of cells with SO flash activity within 3 minutes of time-lapse imaging) plotted as percentage of control condition mean value (n = 3 separate experiments). *p<0.05 and **p<0.001compared to the control value. (**F – H**) The amplitude and kinetics of mitochondrial SO flashes in NPCs. $\Delta F/F_0$ is the amplitude of SO flashes where F_0 refers to basal fluorescence intensity (F); T_p is the time to peak fluorescence intensity (G); and T_{50} is 50% decay time after the peak (H). *p<0.05 versus control (n=3 separate experiments, 80–120 flashes analyzed). (**I**) Global ROS level in NPCs measured using the probe DCF were not changed by treatment with 0.5, 1 µM or 5 µM Aβ1-42 OCP. (n = 3 separate experiments).
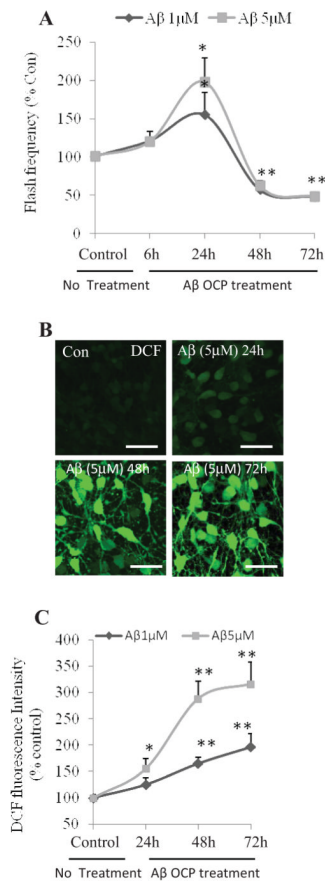
Figure 2. Long-term exposure of NPCs to Aβ1–42 disrupts mitochondrial SO flash generation and increases global ROS production

NPCs in dissociated adherent cell cultures were treated with 1 or 5 μM Aβ1–42 OCP for 24, 48 or 72 h. (**A**) Time course of changes in SO flash incidence. Without OCP treatment (indicated as 0 h), there were $11 \pm 0.3\%$ cells exhibiting flash activity. *p<0.05 and **p<0.001 compared to the control value (0 h). n=3 separate experiments, ~500 cells per condition analyzed. (**B and C**) Representative confocal images of DCF fluorescence in NPCs (B) and results of quantitative analysis of cellular DCF fluorescence intensity (C). Without OCP treatment (control), DCF fluorescence intensity is 647 ± 88 (A.U)/cell. Values for treatment groups are expressed as a percentage of the mean value for the untreated control group. Bar = 20 μm. *p<0.05 and **p<0.001, n=4 experiments, ~500 cells per condition analyzed.
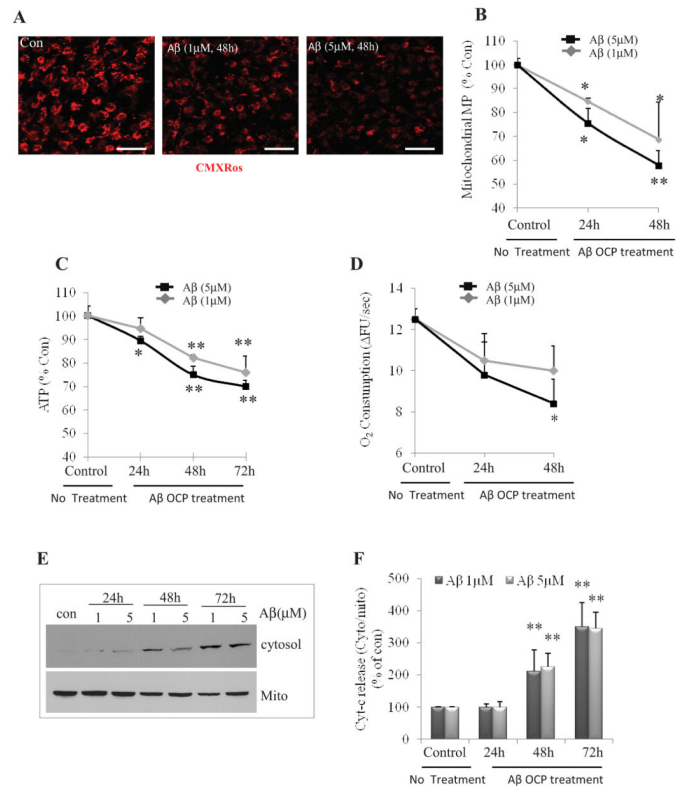
Figure 3. Long-term exposure of NPCs to Aβ1–42 leads to mitochondrial dysfunction
(**A and B**) Representative confocal images (A) and results of quantitative analysis of cellular CMXRos fluorescence intensity (B). Bar = 20 µm. Without OCP treatment (indicated as 0h), the mitotracker red (CMXRos) fluorescence intensity is 2044.0 ± 56.61/cell (A.U.). n=3 separate experiments, ~200 cells per condition analyzed *$p<0.05$, **$p<0.001$ compared to the basal level (time 0). (**C**) Results of analysis of cellular ATP levels. ATP concentration is 510 ± 18.3 pmol/mg proteins. n=4 separate experiments. *$p<0.05$, **$p<0.001$ compared to the control level (No treatment). (**D**) Fluorescence–based determination of oxygen consumption. Result shows the relative oxygen consumption rates for control or Aβ1–42 OCP-treated NPC cultures.**$p<0.05$ compared to the basal level (time 0). n=3 separate experiments. (**E and F**) Representative immunoblot (E) and densitometric analysis (F) showing cytochrome c protein levels in cytosolic and mitochondrial fractions. Values for treatment groups are plotted as a percentage of the mean value for the control untreated group. **p<0.001 compared to the control value (No treatment). n=3 separate experiments.
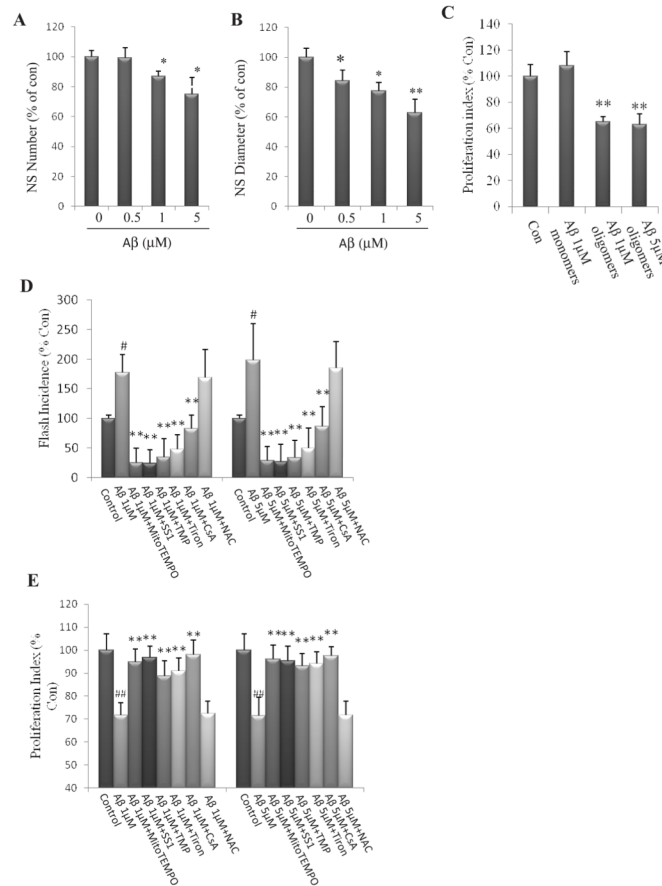
Figure 4. Short-term exposure of NPCs to Aβ1–42 OCP inhibit NPC proliferation
(**A and B**) Neurospheres in cultures prepared from E14.5 mouse cerebral cortex treated for 6 d with vehicle, or 1 or 5 μM Aβ1-42 OCP. Quantitative analysis of neurosphere number (A) and diameter (B) 6 d after exposure to the indicated concentrations of Aβ1-42 OCP. *$p<0.05$, **$p<0.001$ compared to the mean value of control NPCs. n = 3 separate experiments. (**C**) Dissociated adherent NPCs were treated for 24 h with vehicle (con) or the indicated concentrations of Aβ1-42 OCP. Proliferation index (BrdU$^+$cells/total cells) in dissociated adherent NPCs that had been exposed to vehicle (con), Aβ1-42 monomers or Aβ1-42 OCP as indicated (n = 3 separate experiments). *$p<0.05$, **$p<0.001$ compared to the mean value of control NPCs. (**D**) Dissociated adherent NPCs were pretreated for 1 h with 1μM MitoTEMPO, 50 μM SS31, 1μM TMP, 100 μM Tiron, 0.1μM CsA or 1μM NAC, and were then treated for 24 h with 1 or 5μM Aβ1-42 OCP as indicated. Results show analysis of SO flash incidence (number of NPCs which exhibited a mitochondrial SO flash among ~200 cells imaged for 3 minutes. #$p<0.05$, compared to the mean value of control NPCs without Aβ1-42 OCP treatment; **$p<0.001$ compared to the mean value of NPCs treated with Aβ1-42 OCP n = 3 separate experiments. (**E**) Results of analysis of NPC proliferation index (BrdU$^+$cells/total cells) under different conditions (n = 3 separate experiments). ## $p<0.001$ compared to the mean value of control NPCs without Aβ1-42 OCP treatment; **$p<0.001$ compared to the mean value of NPCs treated with Aβ1-42 OCP.
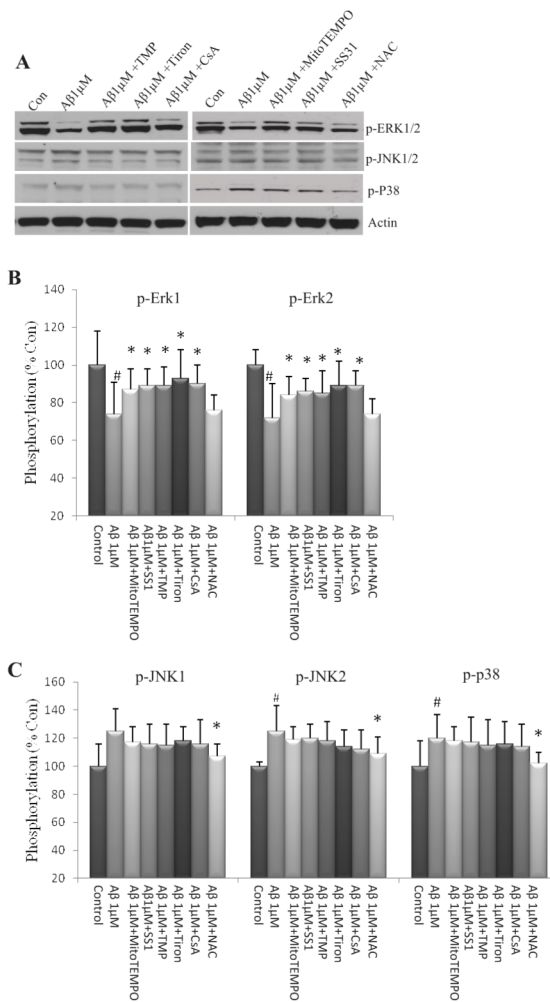
Figure 5. Short-term exposure of NPCs to Aβ1–42 OCP inhibits ERK signaling
Dissociated adherent NPCs were pretreated for 1 h with 1 μM MitoTEMPO, 50 μM SS31, 1 μM TMP, 100 μM Tiron, 0.1μM CsA or 1μM NAC, and were then treated for 24 h with 1μM Aβ1-42 oligomers. Cell lysates were then prepared and subjected to immunoblot anlaysis using antibodies that selectively recognize phosphorylated (active) forms of ERKs 1 and 2, p38 or JNK. Blots were reprobed with phosphorylation-insensitive antibodies against actin. (**A – C**) Representative immunoblot (A) and densitometric analysis (B and C) of NPCs. #$p<0.05$ compared to the mean value of control NPCs without Aβ1-42 OCP treatment; *$p<0.05$ compared to the mean value of NPCs treated with Aβ1-42 OCP. n= 3 separate experiments.

A

B
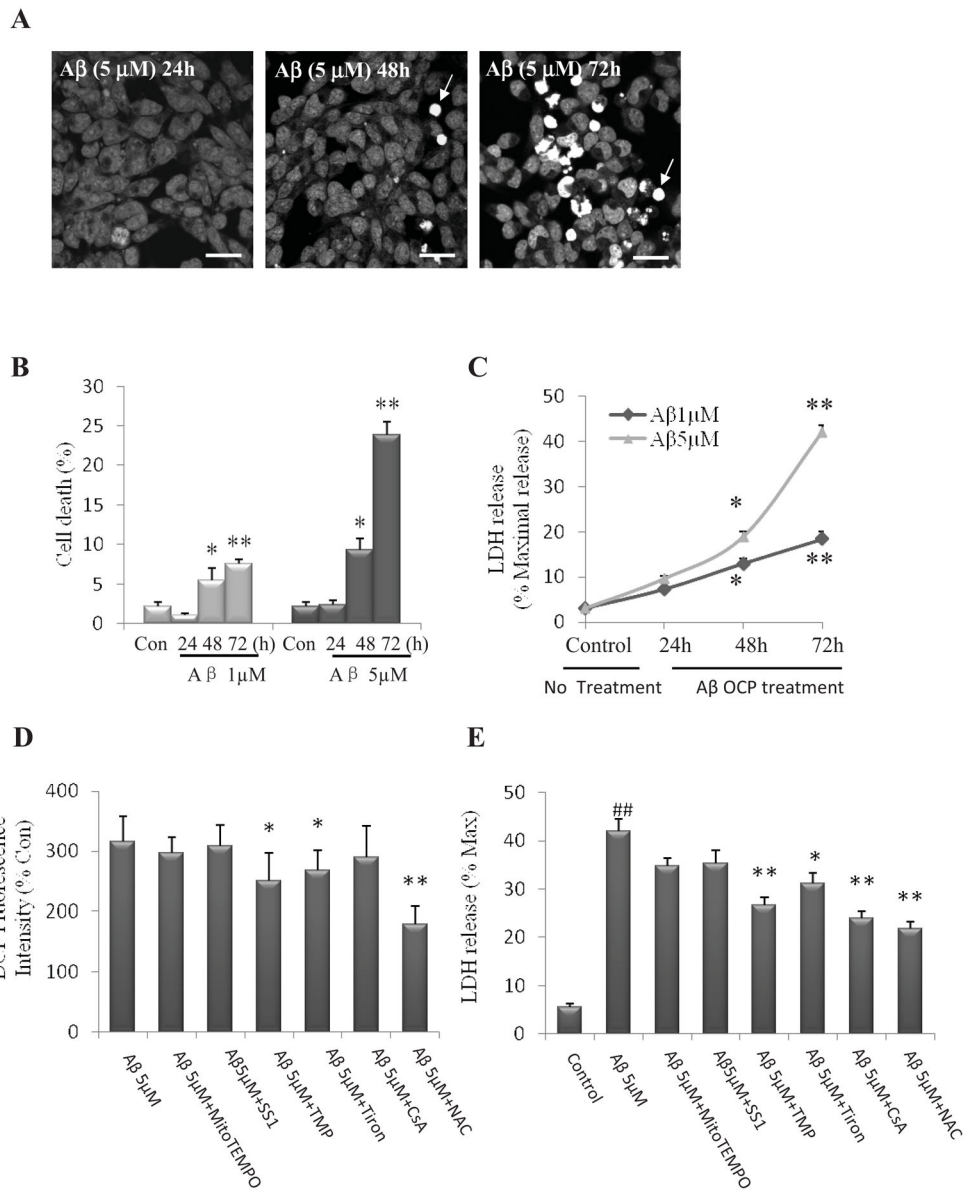

C

D

E

Figure 6. Long-term exposure of NPC to Aβ1–42 results in ROS-mediated death of NPCs
NPCs in dissociated adherent cell cultures were treated with 1 or 5μM Aβ1-42 OCP and at designated time points. (**A**) Representative confocal images showing Hoechst 33258 fluorescence (DNA-binding dye) in NPCs that had been treated with 5 μM Aβ1-42 OCP for 24, 48 or 72 h. Bar = 20μm. (**B**) Results of quantification of NPCs with condensed and fragmented nuclear DNA (considered as dead cells; e.g., arrows). *p<0.05, **$p < 0.001$ compared to the control (No treatment) value. n=3 separate experiments. (**C**) Lactate dehydrogenase (LDH) released from NPCs was determined by measuring LDH activity in the culture medium. *p<0.05, **$p < 0.001$ compared to the control (time 0) value. n=3 separate experiments. Values of treatment groups are plotted as percentage of the mean value of control. (**D and E**) NPCs in dissociated adherent cell cultures were pretreated with 1μM MitoTEMPO, 50 μM SS31, 1μM TMP, 100 μM Tiron, 0.1 μM CsA or 1 μM NAC and then treated with 1 or 5 μM Aβ1-42 oligomers for 72 h. Cellular DCF fluorescence intensity was quantified and the DCF fluorescence intensity for basal untreated control cells is 647±

88 (A.U)/cell (n=4 experiment, ~500 cells per condition analyzed). Values of treatment groups are plotted as percentage of the mean value of control NPCs without Aβ1-42 OCP exposure. *p<0.05, **$p < 0.001$ compared to the mean value of NPCs treated with Aβ1-42 OCP. (D). LDH released from NPCs was determined by measuring LDH activity in the culture medium. ##$p < 0.001$ compared to the mean value of control NPCs without Aβ1-42 OCP treatment; *p<0.05, **$p < 0.001$ compared to the mean value of NPCs treated with Aβ1-42 OCP. n=3 separate experiments. (E).
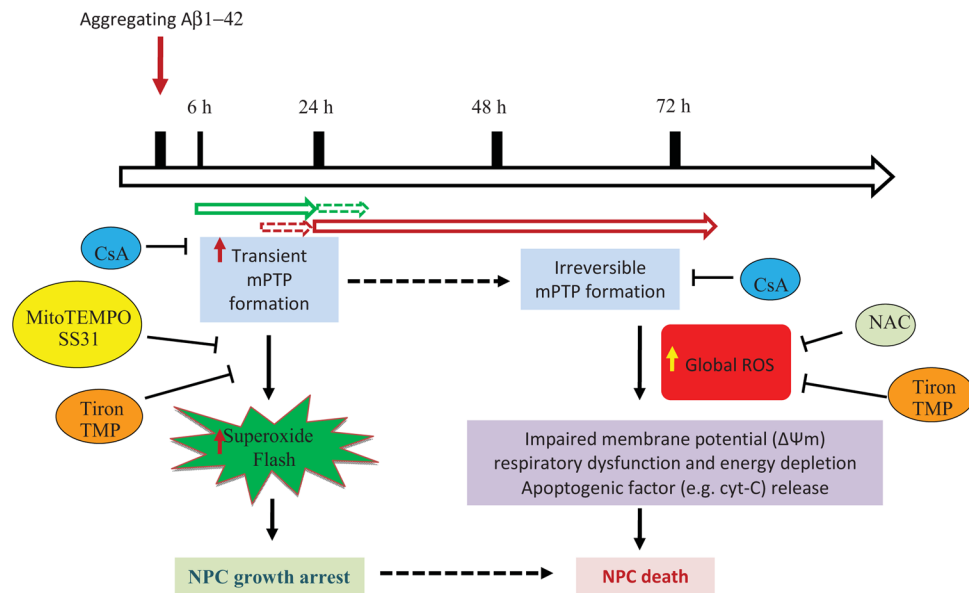
Figure 7. Working model for the roles of mitochondrial SO flashes in the actions of Aβ1-42 on NPC proliferation and survival

Within 6–24 h of exposure to aggregating Aβ1-42 oligomer-containing preparation (OCP) the frequency of mPTP pore opening-mediated mitochondrial SO flashes is increased and causes a reduction in NPC proliferation by a mechanism involving inhibition of ERKs 1 and 2. The increased SO production and the inhibitory effect of Aβ1-42 OCP on NPC proliferation is prevented by cyclosporin A (CsA) an inhibitor of mitochondrial permeability transition pores (mPTP), and by MitoTEMPO and SS31 (mitochondrial SO scavenger), Tiron (a SO scavenger) and TMP (a SO dismutase mimetic agent). Within 48 h of exposure to Aβ1-42 OCP, and continuing through 72 h of exposure, prolonged opening of mPTP occurs, SO flashes cease, the mitochondrial membrane becomes depolarized and ATP production diminishes. An increase of mitochondrial membrane permeability, due in part from mPTP opening, results in the release of cytochrome c from the mitochondria and irreversible progression to cell death.